





Single bead near-infrared random laser based on silica-gel infiltrated with Rhodamine 640

Cite as: J. Appl. Phys. **123**, 133104 (2018); <https://doi.org/10.1063/1.5024934>

Submitted: 05 February 2018 . Accepted: 20 March 2018 . Published Online: 05 April 2018

André L. Moura , Renato Barbosa-Silva, Christian T. Dominguez , Édison Pecoraro , Anderson S. L. Gomes, and Cid B. de Araújo 



View Online



Export Citation



CrossMark

ARTICLES YOU MAY BE INTERESTED IN

[Observation of enhanced infrared absorption in silicon supersaturated with gold by pulsed laser melting of nanometer-thick gold films](#)

Journal of Applied Physics **123**, 133101 (2018); <https://doi.org/10.1063/1.5015984>

[Investigation of in-situ co-doping by Sb and P of germanium films grown on Si\(001\) by molecular beam epitaxy](#)

Journal of Applied Physics **123**, 133102 (2018); <https://doi.org/10.1063/1.5009327>

[Cadmium zinc telluride as a mid-infrared variable retarder](#)

Journal of Applied Physics **123**, 133103 (2018); <https://doi.org/10.1063/1.5020320>

Ultra High Performance SDD Detectors



See all our XRF Solutions

Single bead near-infrared random laser based on silica-gel infiltrated with Rhodamine 640

André L. Moura,^{1,a)} Renato Barbosa-Silva,² Christian T. Dominguez,³ Édison Pecoraro,⁴ Anderson S. L. Gomes,² and Cid B. de Araújo²

¹Grupo de Física da Matéria Condensada, Núcleo de Ciências Exatas–NCEX, Campus Arapiraca, Universidade Federal de Alagoas, 57309-005 Arapiraca, AL, Brazil

²Departamento de Física, Universidade Federal de Pernambuco, 50670-901 Recife, PE, Brazil

³Laboratório de Óptica Biomédica e Imagem, Universidade Federal de Pernambuco, 50740-530 Recife, PE, Brazil

⁴General and Inorganic Chemistry Department, UNESP–São Paulo State University, Institute of Chemistry, 14800-060 Araraquara, SP, Brazil

(Received 5 February 2018; accepted 20 March 2018; published online 5 April 2018)

Photoluminescence properties of single bead silica-gel (SG) embedded with a laser-dye were studied aiming at the operation of near-infrared (NIR) Random Lasers (RLs). The operation of RLs in the NIR spectral region is especially important for biological applications since the optical radiation has deep tissue penetration with negligible damage. Since laser-dyes operating in the NIR have poor stability and are poor emitters, ethanol solutions of Rhodamine 640 (Rh640) infiltrated in SG beads were used. The Rh640 concentrations in ethanol varied from 10^{-5} to 10^{-2} M and the excitation at 532 nm was made by using a 7 ns pulsed laser. The proof-of-principle RL scheme herein presented was adopted in order to protect the dye-molecules from the environment and to favor formation of aggregates. The RL emission from ≈ 650 nm to 720 nm, beyond the typical Rh640 monomer and dimer wavelengths emissions range, was attributed to the trade-off between reabsorption and reemission processes along the light pathways inside the SG bead and the contribution of Rh640 aggregates. *Published by AIP Publishing.* <https://doi.org/10.1063/1.5024934>

I. INTRODUCTION

Random Lasers (RLs), initially proposed by Lethokov¹ and efficiently implemented by Lawandy *et al.*,² in dye-based colloids are currently receiving large attention mainly because of their complex characteristics and potential applications in photonics and medical physics.^{3,4} A large number of studies have been performed with RLs based on different hosts, various gain media, and a large variety of architectures.^{3–8} Presently one goal of large interest is the possibility of obtaining dyes-based RLs emitting beyond the visible spectral range. Near-infrared (NIR) RLs are interesting for biological applications since the optical radiation in this range has a deep tissue penetration and does not produce damage in cells.⁹ Unfortunately, laser-dyes that operate in the NIR present poor stability and low absorption at the standard pump wavelength of 532 nm.^{10,11} Then, in order to overcome this drawback, Cerdan *et al.*¹⁰ reported RL emission in the NIR using a mixture of two dyes. One dye absorbs efficiently the incident radiation and acts as the donor. The second dye is the acceptor which receives the energy transferred from the donor, thereby emitting light with wavelength longer than 650 nm. The energy transfer (ET) mechanism between the donor and acceptor dye molecules was the Förster resonance energy transfer (FRET) process. Another report of long wavelength RL was made by El-Dardiry and Lagendijk¹² with the goal of achieving NIR emission by engineering the laser-dye absorption cross

section. They used a mixture containing a nonfluorescent dye (Quinaldine Blue) and Rhodamine 640 (Rh640). Emission wavelength shifted by a few nanometers due to the change of the Rh640 gain curve caused by the nonfluorescent dye was observed. Another way to obtain shifted RL wavelength is by exploitation of reabsorption/reemission (ReAb/ReEm) processes while the emitted light propagates along the active medium.¹³ In a more recent work,¹⁴ this goal was again addressed and white light emission from a RL based on a mixture of different dyes was reported.

Besides the works in Refs. 10–14, there are other possibilities to control the dye photoluminescence (PL) by changing the electronic structure of the molecules, their mutual interaction, the excitation laser intensity, and the influence of the environment. For instance, by exploiting ET processes between monomers and dimers of Rh640, Barbosa-Silva *et al.*¹⁵ demonstrated bichromatic emission that was tuned by adjusting the energy pulse excitation (EPE) incident on a powder consisting of sub-micrometer silica particles, synthesized by the Stöber modified method,¹⁶ infiltrated with Rh640.

In order to characterize the relevance of the ReAb/ReEm and ET processes to extend the tunability range of dye-based RLs, we investigated the PL characteristics for large concentrations of Rh640 infiltrated in silica-gel (SG) beads. The introduction of dye-molecules in SG beads may be obtained by capillary absorption (post-doping method), when the matrix is embedded in a solution (e.g., ethanol + Rh640), or by introducing the dye molecules at the sol-gel stage of the silica beads preparation (pre-doping method).¹⁷

^{a)}E-mail: andre.moura@fis.ufal.br

In both cases, once the solvent is evaporated, the dye molecules attach to the host matrix by electrostatic interaction or by covalent binding.¹⁷ The formation of Rh640 aggregates inside the SG beads is favored by the interaction among the molecules and the polar surface nature of the host.¹⁸ It is known that increasing the dye concentration leads to formation of fluorescent dimers (J-dimers) until a concentration limit is reached and the J-dimers are gradually converted to non-fluorescent H-dimers.¹⁹ On the other hand, the works reported in Refs. 20–22 indicate that other dyes may present a behavior analogous to Rh640.

Therefore, the results of Refs. 15, 17, and 19–22 lead us to the conclusion that nanoporous SG beads containing Rh640 can be an appropriate hybrid material for RL operation in the NIR. Specifically, SG beads infiltrated with Rh640 may be employed as solid state RL because the feedback necessary for laser action is obtained by a combination of light confinement in the SG nanopores and multiple scattering due to the disordered SG structure. The use of SG beads is also advantageous because the interaction of light with the dielectric particles normally used in RLs, like TiO₂, generates electron-hole (e-h) pairs by two-photon absorption that contributes for fast degradation of the dye molecules due to charge-transfer from the dielectric particles to the dye molecules.^{23,24} In the SG beads, the generation of e-h pairs is not relevant because the silica energy bandgap is larger than twice the energy of the incident photons in the visible range. However, in spite of the large amount of studies related to the PL properties of dyes doped sol-gel samples, only few reports on RL emission were presented.^{15,25–28} For instance, besides the work reported in Ref. 15, Garcia-Revilla *et al.*^{25,26} showed RL with low threshold in a SG powder obtained by grinding SG bulk samples doped with Rhodamine 6G (Rh6G) prepared by the pre-doping method. In Ref. 27 the authors investigate the RL behavior of Rhodamine 610 (Rh610)-TiO₂ nanoparticles confined in a silica xerogel matrix. The concentrations of Rh610 and TiO₂ were adjusted in order to optimize the emission centered at ≈580 nm due to the dye monomers. In Ref. 28, alumina porous ceramic was used as Rhodamine B host, and bi-chromatic emission due to monomers and dimers was observed as in Ref. 15.

In the present paper, we report RL emission from 650 nm to 720 nm observed in SG beads infiltrated by Rh640. The samples were prepared by dropping the SG beads in ethanol solutions of Rh640 with concentrations varying from 10⁻⁵ to 10⁻² M in order to exploit the contribution of aggregates which emits long optical wavelengths. The available literature (see, for instance, Refs. 15, 25, 26, 29, and 30) indicates that the emission in the observed wavelength range (650–720 nm) is not usual for Rh640 based RLs pumped by a 532 nm laser. Therefore, the present report shows an original procedure to exploit ReAb/ReEm and ET processes in order to extend the tunability range of dye-based RLs.

II. EXPERIMENTAL PROCEDURES

A. Samples preparation

Commercially available SG single beads that are almost spherical with average diameter of 1.4 mm were used. The

nanoporosity structure of the beads was characterized using the Brunauer–Emmett–Teller (B.E.T.) technique³¹ and scanning electron microscopy (SEM). It was observed that the SG beads present roughness of ≈50 nm and pores with average diameter of 2.5 nm. The average pore size diameter was determined applying the N₂ adsorption/desorption technique, by using B.E.T.³¹ and the Barret-Joyner-Halenda (B.J.H.) equations³² to isotherm curves relating volume to pressure. Applying these techniques, the N₂ gas is allowed to condense inside the pores, and the sample's fine pore structure can be evaluated. As the pressure increases, the gas condenses first into the pores with the smallest dimensions. The pressure is increased until saturation is reached and then all pores are filled with liquid. Evaluation of the adsorption and desorption branches of the isotherms and the hysteresis between them provide information on the porous size and volume. Further details are given in the [supplementary material](#).

To prepare the samples for RL operation, we soaked the SG beads into an ethanol solution of Rh640 for 24 h. Afterwards, the samples were dried for 5 h at 70 °C to remove the ethanol. At this temperature, the dye molecules are not expected to change their chemical properties, as demonstrated in Ref. 21. The nanoporous constitute the network where the Rh640 molecules are infiltrated. Samples prepared with Rh640 concentrations in ethanol of 10⁻⁵, 10⁻⁴, 5 × 10⁻³, and 10⁻² M were used in the experiments. Formation of Rh640 aggregates occurs for the whole range of concentrations.^{16,17,29}

B. Optical measurements

The experimental setup to excite the SG samples and to collect the PL signals is similar to the ones described in Refs. 15 and 23. The second harmonic of a Q-switched Nd:YAG laser (7 ns, 532 nm) was focused on the center (unless specified) of a single SG bead by a biconvex lens of 10 cm focal distance. The beam area in the focal plane was determined with a charge-coupled device (CCD) camera to be 1.3 × 10⁻⁴ cm². The PL measurements were performed either at 5 Hz pulse repetition rate or single-shot. A pair of polarizers was used to control the EPE incident on the SG bead. The emitted light was collected by a pair of lenses placed along a direction perpendicular to the incident beam direction and sent to a spectrometer that has resolution of 0.75 nm.

III. RESULTS AND DISCUSSION

Figure 1(a) presents a typical SEM image of a SG bead, where the presence of roughness distributed in a random volumetric arrangement is clear. As can be seen in Fig. 1(b), after the ethanol was removed, the SG beads were uniformly colored. The scale is in millimeters, the dye concentration increases from left to right, and the first sphere on the left does not contain Rh640.

Figures 2(a)–2(d) show the PL spectra, corresponding to Rh640 concentrations of 10⁻⁵, 10⁻⁴, 5 × 10⁻³, and 10⁻² M in ethanol, for various EPE values. The spectra in Fig. 2(a), corresponding to 10⁻⁵ M, are typical of Rh640 with central wavelength at ≈620 nm and a tail extending to ≈650 nm. No

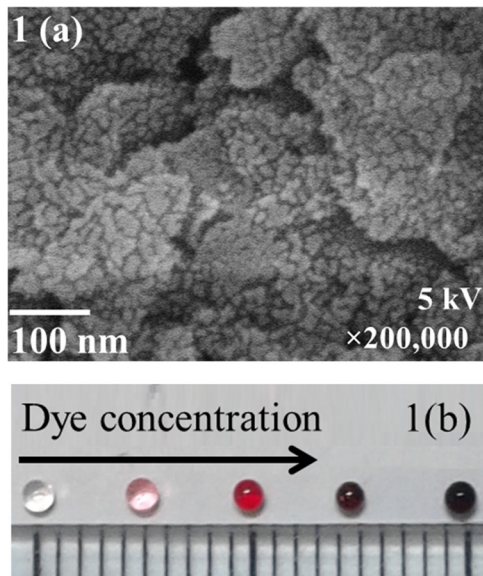


FIG. 1. (a) Image of a silica gel (SG) bead surface obtained by scanning electron microscopy. (b) Photograph of SG beads containing different Rh640 concentrations after the ethanol was removed. The first sphere from left to right does not contain Rh640; the other beads correspond to various starting Rh640 in ethanol solutions (concentrations of 10^{-5} , 10^{-4} , 5×10^{-3} , and 10^{-2} M, from left to right). The scale is in millimeter.

RL action was observed in this case. For concentrations larger than 10^{-5} M, the spectra exhibit the characteristic RL behavior, that is bandwidth narrowing and enhancement in the slope efficiency as the EPE is increased, as discussed below. Notice that the PL spectra change as a function of Rh640 concentration and excitation laser intensity. Figure 2(b) shows that when the concentration is 10^{-4} M, the maximum RL amplitude occurs at ≈ 660 nm, a wavelength which is the characteristic of dimers emission. On the other hand,

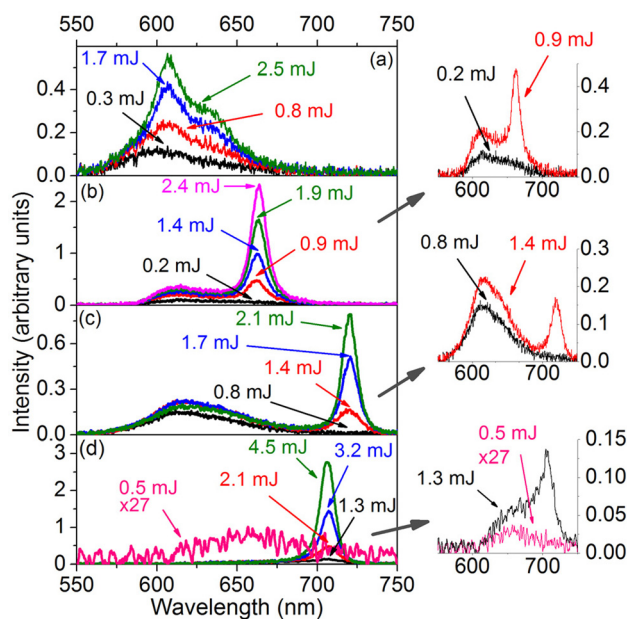


FIG. 2. Spectral dependence of the emitted photoluminescence (PL) versus the excitation pulse energy (EPE), for different starting Rh640 concentrations: (a) 10^{-5} M, (b) 10^{-4} M, (c) 5×10^{-3} M, and (d) 10^{-2} M. The insets in (b)–(d) are the PL spectra for EPE smaller and near the threshold.

Figs. 2(c) and 2(d) show the spectra for concentrations of 5×10^{-3} and 10^{-2} M, and the RL emissions are centered around 720 and 710 nm, respectively, beyond the dimer's characteristic emission range. The blue RL wavelength shift when the dye concentration is increased from 5×10^{-3} and 10^{-2} M is essentially due to the position of the incident beam onto the bead surface, as discussed below.

The absence of spikes in the RL spectra, sometimes attributed to a non-resonant feedback in which light propagates in a diffusive mode as originally proposed by Letokhov,¹ does not necessarily mean the absence of resonant modes inside the scattering material. The RL spectra shown in Fig. 2 are smooth without spikes due to the superposition of a large number of resonant RL modes inside the investigated spectral resolution, as well-described in Refs. 33–35. However, an evidence of RL emission, distinguished from the amplified spontaneous emission, is shown in Fig. 3(b) by the threshold behavior, i.e., enhancement in the slope efficiency as the EPE is increased. It is worth emphasizing the presence of spikes does not necessarily mean the existence of resonant modes since, in the low scattering regime, the spikes can be due to rare long paths associated with Lévy flights of photons in the gain region inferred by the observation of non-Gaussian heavy-tailed intensity distribution as deeply investigated in Ref. 36. Although the mean free path could not be determined in the beads by using, for example,

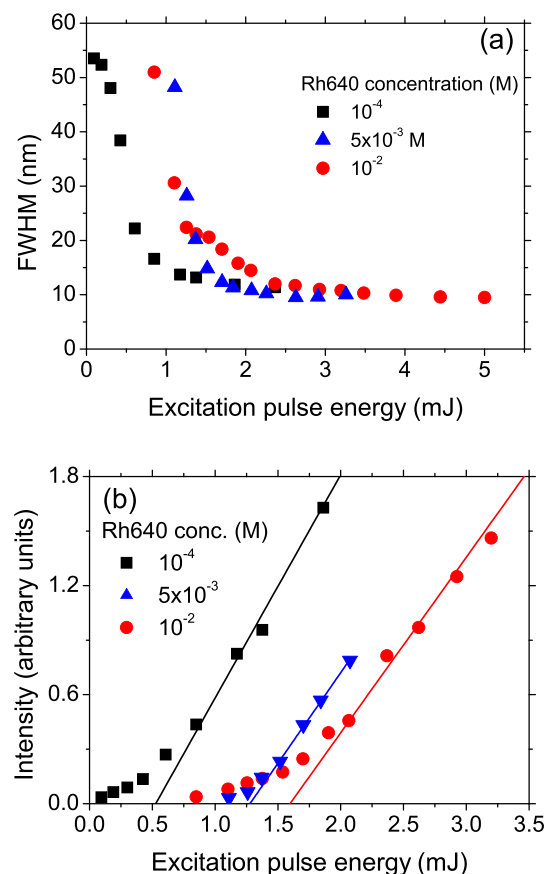


FIG. 3. Observed behavior for starting Rh640 concentrations of 10^{-4} , 5×10^{-3} , and 10^{-2} M versus the excitation pulse energy (EPE): (a) Full width at half maximum (FWHM); (b) intensity dependence of the random laser.

the coherent backscattering technique,³⁷ due to technical difficulties like the small size and nonplanar shape of the beads, the absence of spikes and the threshold behavior assure that the photon transport mean free path is of the same order of magnitude as the RL wavelength supporting high scattering strengths.

Figure 3(a) shows the full width at half maximum (FWHM) of the emission band as a function of the EPE for Rh640 concentrations of 10^{-4} M, 5×10^{-3} M, and 10^{-2} M, while Fig. 3(b) shows the dependence of the PL intensity versus the EPE. The bandwidth narrowing and the abrupt change of the PL intensity as the EPE increases provide RL thresholds of 0.53 mJ (10^{-4} M), 1.25 mJ (5×10^{-3} M), and 1.60 mJ (10^{-2} M). The results for all Rh640 concentrations are summarized in Table I. The smaller slope efficiency in Fig. 3(b) and the higher EPE threshold as the Rh640 concentration increases are due to the conversion of J-dimers to non-fluorescent H-dimers.^{19,20} Accordingly, although all the range of EPE was not exploited in characterizing the 5×10^{-3} M, extrapolation of the corresponding linear fit displayed in Fig. 3(b) indicates that the maximum RL intensity is in between the ones for 10^{-4} and 10^{-2} M samples. There is an interplay between the increase in dye concentration and decrease in the absorption length that implies in a small gain volume which compensates the luminescence quenching due to the formation of non-fluorescent aggregates at high dye concentration.

The spectral behavior shown in Fig. 2 is influenced by ReAb/ReEm processes due to the large molecules concentration obtained after removing the ethanol from the samples, the presence of aggregates, and the multiple scattering provided by the nanoporous network within the highly disordered SG bead structure. The longer wavelength emission associated with the Rh640 aggregates is understood considering the following two possible mechanisms. In one mechanism, monomers or dimers promoted to excited states can relax to the ground state by emitting photons that are absorbed by aggregates which emit longer wavelengths. In the second mechanism, NIR emission occurs due to the ET from the excited monomers or dimers to the fluorescent aggregates.²⁹ We emphasize that a large ET probability to the aggregates enabled by the FRET mechanism is expected, ensured by the high concentration of Rh640 inside the SG bead. For high Rh640 concentrations in the ethanol solution (5×10^{-3} and 10^{-2} M), the number of aggregates is very large and consequently the PL from the monomers or dimers

TABLE I. Random laser excitation pulse energy (EPE) threshold, the corresponding intensity threshold, and the minimum bandwidth for different Rhodamine 640 concentrations.

Rh640 concentration (M)	EPE threshold (mJ)	Intensity threshold (MW/cm ²)	Minimum bandwidth (nm)
10^{-5}
10^{-4}	0.53	570	11.4
5×10^{-3}	1.25	1370	9.5
10^{-2}	1.60	1760	9.5

is quenched due to ET to the Rh640 aggregates as evidenced by the darkness of the more concentrated samples in Fig. 1(b). Owing to the nanoporous network, the light pathways inside a SG bead can be long due to the multiple scattering. Moreover, due to the overlap between the absorption and emission cross section spectra of monomers, dimers, and larger aggregates, and their spatial proximities, ET processes are more probable here than in the experiments performed in solutions^{13,29} implying in RL wavelengths larger than the typical 650 nm wavelength observed for Rh640 monomers and dimers. We recall that Álvarez *et al.*³⁸ also found that the growth of an observed band of long wavelength in dipyrromethene dyes incorporated into solid polymeric media was due to ReAb/ReEm processes together with the contribution of vibronic transitions.

Figure 4(a) shows the RL spectra for a SG bead prepared with Rh640 concentration of 10^{-2} M and a powder obtained after grinding the same SG bead. Note that the RL peak is shifted from ≈ 710 nm to ≈ 650 nm indicating that in the powder the effective light pathway is shorter than inside the porous network of the bulk SG bead. Also, it suggests that in the powder, the contributions due to vibronic transitions and the large Rh640 aggregates become relatively less important than inside the bulk bead. Figure 4(b) presents the RL

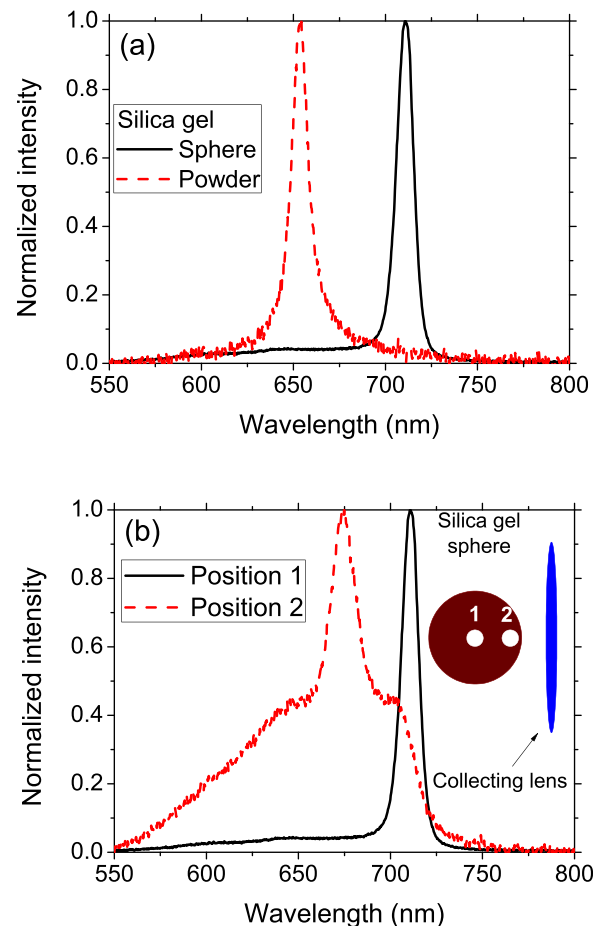


FIG. 4. Normalized intensity spectrum for starting Rh640 concentration of 10^{-2} M: (a) for a single SG bead and for a powder obtained grinding the SG bead; (b) for excitation in the positions 1—in the center and 2—near the edge of the SG bead.

spectra for excitation in two different positions of a single SG bead. The excitation laser was focused in the positions 1 or 2, as indicated in the figure, and the PL is collected by a lens located besides the bead as indicated in Fig. 4(b). The PL wavelength for excitation at the position 1 was centered at ≈ 710 nm, while the emission for excitation at the position 2 was centered at ≈ 675 nm. The wavelength shift of ≈ 35 nm corroborates the interpretation that the emission at longer wavelengths is highly determined by the ReAb/ReEm process because the PL pathway inside the bead is longer for excitation in the position 1. This result indicates a new possibility for operation of wavelength tunable dye-based RLs over large spectral range by tailoring the beads' shape and their size, and resorting to pump engineering. Another remarkable point in the present results is the RL wavelength blue shift observed in Fig. 2(d) for EPE larger than 2.1 mJ. This effect, attributed to the influence of excited state absorption in Ref. 39, will be the subject of future work.

IV. CONCLUSION

In summary, near-infrared random laser emitted by nanoporous silica-gel single beads infiltrated with Rh640 was demonstrated. The excitation pulse energy threshold, the minimum bandwidth observed, and the central wavelength were dependent on the Rh640 concentration and on the light pathway inside the beads. The samples were prepared by infiltrating ethanol solutions of Rh640 with concentrations from 10^{-5} to 10^{-2} M into silica-gel beads having dimensions in the millimeter range. The samples exhibited RL emission from 670 nm to ≈ 720 nm due to reabsorption/reemission processes involving the Rh640 molecules and their aggregates, as well as the multiple scattering of light provided by the porous network inside the SG beads. The results also indicate that the tunability range of dye-based RLs can be extended by shaping the hosting SG bead or by pumping engineering using the methods already applied to other systems,^{40–42} where shaping the spatial intensity distribution of the excitation light allows RL single-mode operation. The present results can motivate RL studies using large dye concentrations that have been avoided due to the decrease in the fluorescence quantum yield by the formation of non-fluorescent aggregates.

SUPPLEMENTARY MATERIAL

See [supplementary material](#) for detailed description of the methods used to determine the porous size and volume of SG beads.

ACKNOWLEDGMENTS

We acknowledge financial support from the Brazilian agencies Conselho Nacional de Desenvolvimento Científico e Tecnológico (CNPq) and the Fundação de Amparo à Ciência e Tecnologia do Estado de Pernambuco (FACEPE). This work was performed in the framework of the National Institute of Photonics (INCT de Fotônica) project and PRONEX/CNPq/FACEPE. A.L.M. thanks CNPq and FAPEAL for financial support.

- ¹V. S. Letokhov, JETP Lett. **5**, 212 (1967).
- ²N. M. Lawandy, R. M. Balachandran, A. S. L. Gomes, and E. Sauvain, *Nature* **368**, 436 (1994).
- ³M. Noginov, *Solid-State Random Lasers* (Springer, New York, 2005).
- ⁴F. Luan, B. B. Gu, A. S. L. Gomes, K. T. Yong, S. C. Wen, and P. N. Prasad, *Nano Today* **10**, 168 (2015).
- ⁵C. J. S. de Matos, L. de S. Menezes, A. M. Brito-Silva, M. A. M. Gámez, A. S. L. Gomes, and C. B. de Araújo, *Phys. Rev. Lett.* **99**, 153903 (2007).
- ⁶V. Folli, A. Puglisi, L. Leuzzi, and C. Conti, *Phys. Rev. Lett.* **108**, 248002 (2012).
- ⁷C. T. Dominguez, Y. Lacroute, D. Chaumont, M. Sacilotti, C. B. de Araújo, and A. S. L. Gomes, *Opt. Express* **20**, 17380 (2012).
- ⁸M. A. S. de Oliveira, C. B. de Araújo, and Y. Messaddeq, *Opt. Express* **19**, 5620 (2011).
- ⁹H. P. Berlien, H. Breuer, G. J. Müller, N. Krasner, T. Okunata, and D. Sliney, *Applied Laser Medicine* (Springer Science + Business Media, 2012).
- ¹⁰L. Cerdán, E. Enciso, V. Martín, J. Bañuelos, I. López-Arbeloa, A. Costela, and I. García-Moreno, *Nat. Photonics* **6**, 621 (2012).
- ¹¹U. Brackmann, *Lambdachrome® Laser Dyes* (Lambda Physics, 2000).
- ¹²R. G. S. El-Dardiry and A. Lagendijk, *Appl. Phys. Lett.* **98**, 161106 (2011).
- ¹³M. A. F. de Souza, A. Lencina, and P. Vaveliuk, *Opt. Lett.* **31**, 1244 (2006).
- ¹⁴S. Chen, X. Zhao, Y. Wang, J. Shi, and D. Liu, *Appl. Phys. Lett.* **101**, 123508 (2012).
- ¹⁵R. Barbosa-Silva, A. F. Silva, A. M. Brito-Silva, and C. B. de Araújo, *J. Appl. Phys.* **115**, 43515 (2014).
- ¹⁶C. A. R. Costa, C. A. P. Leite, and F. Galembeck, *J. Phys. Chem. B* **107**, 4747 (2003).
- ¹⁷C. M. Carbonaro, *J. Photochem. Photobiol. A* **222**, 56 (2011).
- ¹⁸C. M. Carbonaro, A. Anedda, S. Grandi, and A. Magistri, *J. Phys. Chem. B* **110**, 12932 (2006).
- ¹⁹P. Innocenzi, H. Kozuka, and T. Yoko, *J. Non Cryst. Solids* **201**, 26 (1996).
- ²⁰C. M. Carbonaro, F. Meinardi, P. C. Ricci, M. Salis, and A. Anedda, *J. Phys. Chem. B* **113**, 5111 (2009).
- ²¹S. Grandi, C. Tomasi, P. Mustarelli, F. Clemente, and C. M. Carbonaro, *J. Sol-Gel Sci. Technol.* **41**, 57 (2007).
- ²²B. Samiey and A. R. Toosi, *J. Hazard. Mater.* **184**, 739 (2010).
- ²³A. M. Brito-Silva, A. Galembeck, A. S. L. Gomes, A. J. Jesus-Silva, and C. B. de Araújo, *J. Appl. Phys.* **108**, 033508 (2010).
- ²⁴E. Jimenez-Villar, V. Mestre, P. C. de Oliveira, and G. F. de Sá, *Nanoscale* **5**, 12512 (2013).
- ²⁵S. García-Revilla, J. Fernández, M. A. Illarramendi, B. García-Ramiro, R. Balda, H. Cui, M. Zayat, and D. Levy, *Opt. Express* **16**, 12251 (2008).
- ²⁶S. García-Revilla, M. Zayat, R. Balda, M. Al-Saleh, D. Levy, and J. Fernández, *J. Opt. Express* **17**, 13202 (2009).
- ²⁷F. J. Al-Maliki, *Adv. Mater. Phys. Chem.* **2**, 110 (2012).
- ²⁸S. J. Marinho, L. M. Jesus, L. B. Barbosa, D. R. Ardila, M. A. R. C. Alencar, and J. J. Rodrigues, *Laser Phys. Lett.* **12**, 055801 (2015).
- ²⁹P. Vaveliuk, A. M. de Brito-Silva, and P. C. de Oliveira, *Phys. Rev. A* **68**, 13805 (2003).
- ³⁰F. Bos, *Appl. Opt.* **20**, 1886 (1981).
- ³¹S. Brunauer, P. H. Emmett, and E. Teller, *J. Am. Chem. Soc.* **60**, 309 (1938).
- ³²E. P. Barrett, L. G. Joyner, and P. P. Halenda, *J. Am. Chem. Soc.* **73**, 373 (1951).
- ³³S. García-Revilla, J. Fernández, M. Barredo-Zuriarrain, L. D. Carlos, E. Pecoraro, I. Iparraguirre, J. Azkargorta, and R. Balda, *Opt. Express* **23**, 1456 (2015).
- ³⁴N. Ghofraniha, I. Viola, F. Di Maria, G. Barbarella, G. Gigli, L. Leuzzi, and C. Conti, *Nat. Commun.* **6**, 6058 (2015).
- ³⁵S. García-Revilla, J. Fernández, M. Barredo-Zuriarrain, L. D. Carlos, E. Pecoraro, I. Iparraguirre, J. Azkargorta, and R. Balda, *Adv. Dev. Mater.* **1**, 38 (2015).
- ³⁶E. Ignesti, F. Tommasi, L. Fini, S. Lepri, V. Radhalakshmi, D. Wiersma, and S. Cavalieri, *Phys. Rev. A* **88**, 033820 (2013).
- ³⁷G. Labeyrie, C. A. Muller, D. S. Wiersma, C. Miniatura, and R. Kaiser, *J. Opt. B* **2**, 672 (2000).

- ³⁸M. Álvarez, A. Costela, I. García-Moreno, F. Amat-Guerri, M. Liras, R. Sastre, F. López Arbeloa, J. Bañuelos Prieto, and I. López Arbeloa, *J. Appl. Phys.* **101**, 113110 (2007).
- ³⁹M. A. Noginov, H. J. Caulfield, N. E. Noginova, and P. Venkateswarlu, *Opt. Commun.* **118**, 430 (1995).

- ⁴⁰N. Bachelard, S. Gigan, X. Noblin, and P. Sebbah, *Nat. Phys.* **10**, 426 (2014).
- ⁴¹M. Leonetti and C. López, *Appl. Phys. Lett.* **102**, 071105 (2013).
- ⁴²J. Andreasen, N. Bachelard, S. B. N. Bhaktha, H. Cao, P. Sebbah, and C. Vanneste, *Int. J. Mod. Phys. B* **28**, 1430001 (2014).